ROYAL SOCIETY
OF CHEMISTRY

PAPER

Check for updates

Enhancing the antivirus activity of chimeric canine interferon with ricin subunit B by using nanoparticle formulations

Chengbiao Sun, [ID] †[a] Mingxin Dong,†[a] Yucong Song,[c] Jianxu Zhang,[a] Yan Wang,[a] Ying Chang,[b] Haotian Yu,[a] Na Xu,*[b] Zhigang Xie [ID] *[c] and Wensen Liu*[a]

Despite interferon alpha having a broad spectrum of antiviral activity and strong antiproliferative activity, its applications are severely limited due to the intrinsic properties of proteins, such as poor stability and short serum half-life. In our study, canine interferon alpha (CaIFNα) gene was fused with the ricin toxin B chain (RTB) to form rCaIFNα/RTB, which encodes a 463-amino acid protein containing a 15-amino acid encoded $(G_4S)_3$ flexible linker. After expression in prokaryote, purification and renaturation, the cytotoxicity and antiviral activity of rCaIFNα/RTB were investigated in Madin–Darby canine kidney (MDCK) cells. rCaIFNα/RTB exerted a superior anti-vesicular stomatitis virus (VSV) activity on MDCK cells. Furthermore, we have developed a nanoparticle formulation of rCaIFNα/RTB by using polyethylenimine (PEI) through electrostatic interaction. rCaIFNα/RTB@PEI$_{10000}$ is more stable than rCaIFNα/RTB at various pH and temperature levels, and it possesses enhanced antiviral activity. Our findings facilitate further research on the role of type I IFN in antiviral defense responses in Canis lupus familiaris.

Introduction

Interferons (IFNs) were first reported as a substance that interferes with vaccinia and influenza virus replication.[1] Soon after confirmation of their broad spectrum of antiviral activity, several studies also demonstrated their strong antiproliferative and immune-modulatory activities. Type I IFNs bind to ubiquitous membrane receptors,[2] which are formed by a heterodimer of two transmembrane proteins (IFNαR1, IFNαR2), triggering the IFNAR-JAK-STAT signaling cascade, thus inducing the production of a wide array of antiviral proteins, including products of the "classical" IFN-stimulated genes (ISGs).[3–5]

The production of the first recombinant human (rh) type I IFN proteins in Escherichia coli in 1980 raised hope in the therapy of different neoplastic and viral diseases.[6] Especially in recent years, interferon therapy in viral diseases such as hepatitis B, hepatitis C and the treatment of cancer has achieved good curative effects.[7,8] However, because of its poor stability and short serum half-life, the usual dose for unmodified IFNα is required to be once daily or three times weekly to achieve its

medical performance, which leads to an increase in the frequency and severity of adverse effects. To improve its pharmacokinetics and decrease the dosing frequency, several formulations have been developed to protract the effect of IFN, including biodegradable microspheres,[9] multivesicular liposomes,[10] and molecular modification with poly(ethylene glycol) (PEG; PEGylation).[11] Several PEGylated rhIFN products are already in the market because of their prolonged half-life.[12] However, the chemical conjugation process of PEGylation is rather complex and involves generating new molecular entities, and their safety evaluation is a long process. It has been revealed that the bioactivity of the protein may be affected to some extent. Hence, some studies presented an alternative strategy to PEGylation. A genetic fusion chimeric protein was expressed, composed of recombinant interferon α and recombinant human serum albumin, and it exhibits similar antiviral and antiproliferative activities and a protracted serum half-life compared with unmodified interferon α.[13,14]

In this study, we first expressed a chimeric canine interferon alpha fused with ricin toxin B subunit (rCaIFNα/RTB) in E. coli and tested its biological activity in vitro. Ricin toxin B subunit is one subunit of the ricin toxin, which possesses extremely fatal toxicity. RTB is a 34-kD galactose-binding lectin which could bind to cell-surface glycoproteins or glycolipids, mediate cell endocytosis, and deliver the ricin A subunit into cytosol to exert its toxic activity.[15–17] Studies have shown that RTB is non-toxic and could be a superior drug carrier when fused with other molecules.[18–22] Furthermore, our present study investigated the immune-modulatory effects of RTB on the murine macrophage

[a]Institute of Military Veterinary Medicine, Academy of Military Medical Sciences, Key Laboratory of Jilin Province for Zoonosis Prevention and Control, Changchun, 130122, P. R. China. E-mail: liuws85952@163.com

[b]Jilin Medical University, Jilin, 132013, P. R. China. E-mail: xunajlu@sina.com

[c]State Key Laboratory of Polymer Physics and Chemistry, Changchun Institute of Applied Chemistry, China Academy of Sciences, Changchun, 130022, P. R. China. E-mail: xiez@ciac.ac.cn

† C. Sun and M. Dong contributed equally to this work.

cell line RAW264.7, finding that RTB could activate macrophages and release downstream cascades of JAK-STAT. Phosphorylation levels were increased at 20 sites in the RTB-treated macrophage cell line,[23] including JAK1/TYK2 and STAT1/2, which are the docking sites and specific adapter protein of the type 1 interferon signaling pathway.

Polyethylenimine (PEI) is a cationic polymer that has been used for many years in typical industrial processes, such as paper production, shampoo production, and water purification.[24] Since 1995 when PEI was first introduced as a multipurpose vector for gene delivery, it has been widely utilized as nanocarrier for gene delivery systems, such as RNA delivery[25–28] and chemotherapy.[29–32] Our study investigated the potential of PEI as a nanocarrier for rCaIFNα/RTB, and the antiviral activity and physiochemical characteristics of the nanoparticle formulation were evaluated as well.

As shown in Fig. 1, recombinant CaIFNα/RTB chimeric protein was expressed and co-assembled with polymer PEI_{10000}. The formed $rCaIFNα/RTB@PEI_{10000}$ nanoparticles disintegrated after entering the inner environment of the organism, and rCaIFNα was slowly released, recognized by the cell surface type I interferon receptor to activate the downstream IFN-JAK-STAT signaling cascade, which leads to the expression of the interferon-stimulated gene to develop interferon α's broad-spectrum antiviral effect.

Results and discussion

Prokaryotic expression of rCaIFNα/RTB

To ensure optimal flexibility or separation of the adjacent domains and to promote intermolecular interactions of engineered fusion proteins,[33] glycine–serine (GS) linkers were introduced to express canine interferon fusion protein, which was fused with the ricin subunit B chain. Glycine–serine (GS) linkers have no ordered secondary structure and could be adjusted by the number (n) of G_4S-units. $(G_4S)n$-linkers are frequently used in recombinant fusion proteins and antibody engineering to generate loops that connect domains and do not interfere with their folding.[34,35] The gene fragment of interest encoding the rCaIFNα/RTB protein was modified as shown in Fig. 2 and cloned into the pET28a expression vector. Then, the recombinant expression vector was transformed into *E. coli*/BL21(DE3) and induced with 1 mmol L^{-1} IPTG. After denaturation–purification–renaturation processes, the rCaIFNα/RTB
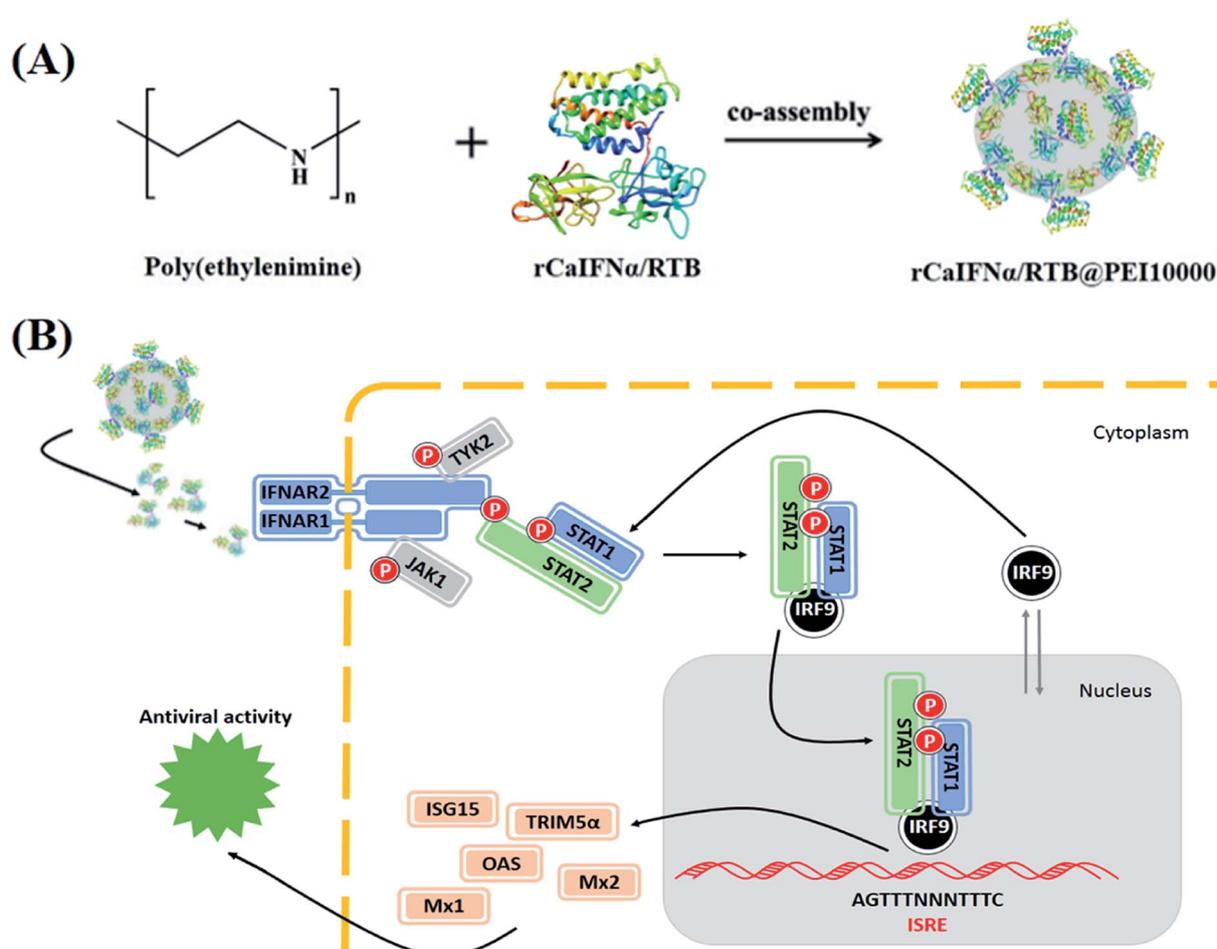

Fig. 1 Schematic illustration of $rCaIFNα/RTB@PEI_{10000}$. (A) Development scheme of $rCaIFNα/RTB@PEI_{10000}$. (B) Antiviral mechanism of $rCaIFNα/RTB@PEI_{10000}$.

Gene Processing

Feature Key	Position	Description	Graphical View	Length
Gene I	1-435	Canine Interferon α		435
Gene II	436-540	$(G_4S)_3$ Linker		45
Gene III	541-1329	Ricin B chain		789

Fig. 2 Gene processing of recombinant CaIFNα/RTB.

protein was folded in the correct structure, which coded for 463 amino acids. SDS-PAGE analysis revealed that the rCaIFNα/RTB was mainly expressed as an inclusion body form, with an apparent molecular weight of 51 kD (Fig. 3A). Western blot analysis of the inclusion bodies incubated with 6-polyhistidine rabbit monoclonal antibody and HRP goat anti-rabbit IgG indicated that the *CaIFNα/RTB* gene was expressed, consistent with the SDS-PAGE results (Fig. 3B).

Synthesis and characterization of rCaIFNα/RTB@PEI$_{10000}$ NPs

Despite the main applications of PEI polymer as a gene vector for medical applications,[36–40] our study assembled the recombinant protein and PEI to enhance the antiviral activity of rCaIFNα/RTB. The rCaIFNα/RTB@PEI$_{10000}$ NPs were synthesized by mixing rCaIFNα/RTB and PEI$_{10000}$ in a water solution, followed by centrifugation and washing. The recombinant protein was dialyzed in Tris–HCl buffer with pH value 9.5, which is over the theoretical PI of rCaIFNα/RTB, to display negative charge and maximize the electrostatic absorption effect of PEI polymer. rCaIFNα/RTB@PEI$_{10000}$ NPs were further characterized by TEM and zeta potential techniques. The morphology and structure of rCaIFNα/RTB@PEI$_{10000}$ NPs were firstly investigated by TEM. As shown in Fig. 4A, as expected, the rCaIFNα/RTB@PEI$_{10000}$ NPs presented a uniform spherical shape, with the average size of 332.4 nm, as shown in Fig. 4D.

Zeta potential of rCaIFNα/RTB@PEI$_{10000}$ NPs was also monitored to estimate whether the rCaIFNα/RTB was co-assembled with PEI. Our results showed that compared with −16.7 mV of rCaIFNα/RTB, +30.4 mV zeta potential was observed for the rCaIFNα/RTB@PEI$_{10000}$ (Fig. 4C). Then, the successful co-assembly of rCaIFNα/RTB with PEI polymer was examined by sodium dodecyl sulfate polyacrylamide gel electrophoresis (SDS-PAGE). Free rCaIFNα/RTB without PEI was used as parallel control. Fig. 4B shows the two proteins displaying the main band with same molecular weight at 51 kD. All of these results mentioned above indicate that the rCaIFNα/RTB was successfully assembled with the PEI polymer.

The stability of rCaIFNα/RTB@PEI$_{10000}$ NPs

The stability of rCaIFNα/RTB@PEI$_{10000}$ NPs was tested by monitoring their size and size distribution in aqueous solution at 4 °C for 6 days. As shown in Fig. 4E, rCaIFNα/RTB@PEI$_{10000}$ NPs remained stable and monodispersed for up to 6 days in aqueous solution at 4 °C, guaranteeing the feasibility of long-term storage.

Cellular uptake of rCaIFNα/RTB@PEI$_{10000}$ NPs

To better observe the cellular uptake process of NPs, FITC was selected as a fluorescence probe to label rCaIFNα/RTB, and FITC-rCaIFNα/RTB@PEI$_{10000}$ was prepared. The green fluorescence emitted under excitation was used to better observe the uptake of
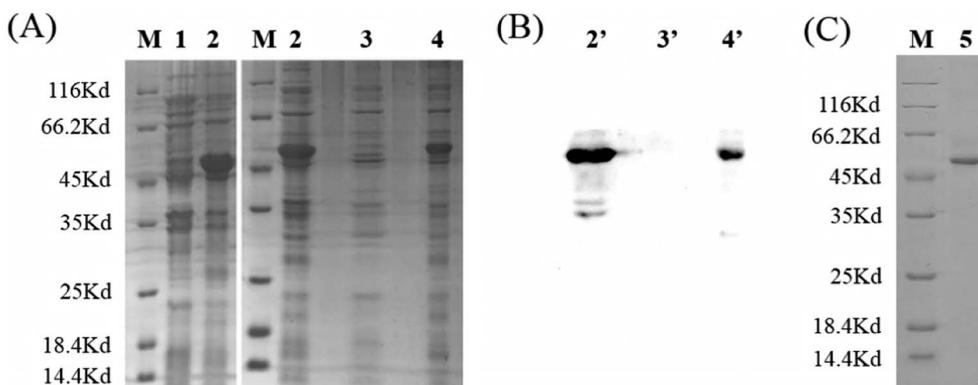

Fig. 3 (A) Protein expression and verification of rCaIFNαRTB. M: unstained protein marker; lane 1: empty vector pET28a; 2: rCaIFNαRTB with 1 mM IPTG induction; 3: supernatants of rCaIFNαRTB; 4: precipitates of rCaIFNαRTB. (B) Western blot analysis of rCaIFNαRTB by anti-6×His Tag monoclonal antibodies. 2′: rCaIFNαRTB with 1 mmol L^{-1} IPTG induction; 3′: supernatants of rCaIFNαRTB; 4′: precipitates of rCaIFNαRTB. (C) rCaIFNαRTB after purification and renaturation.

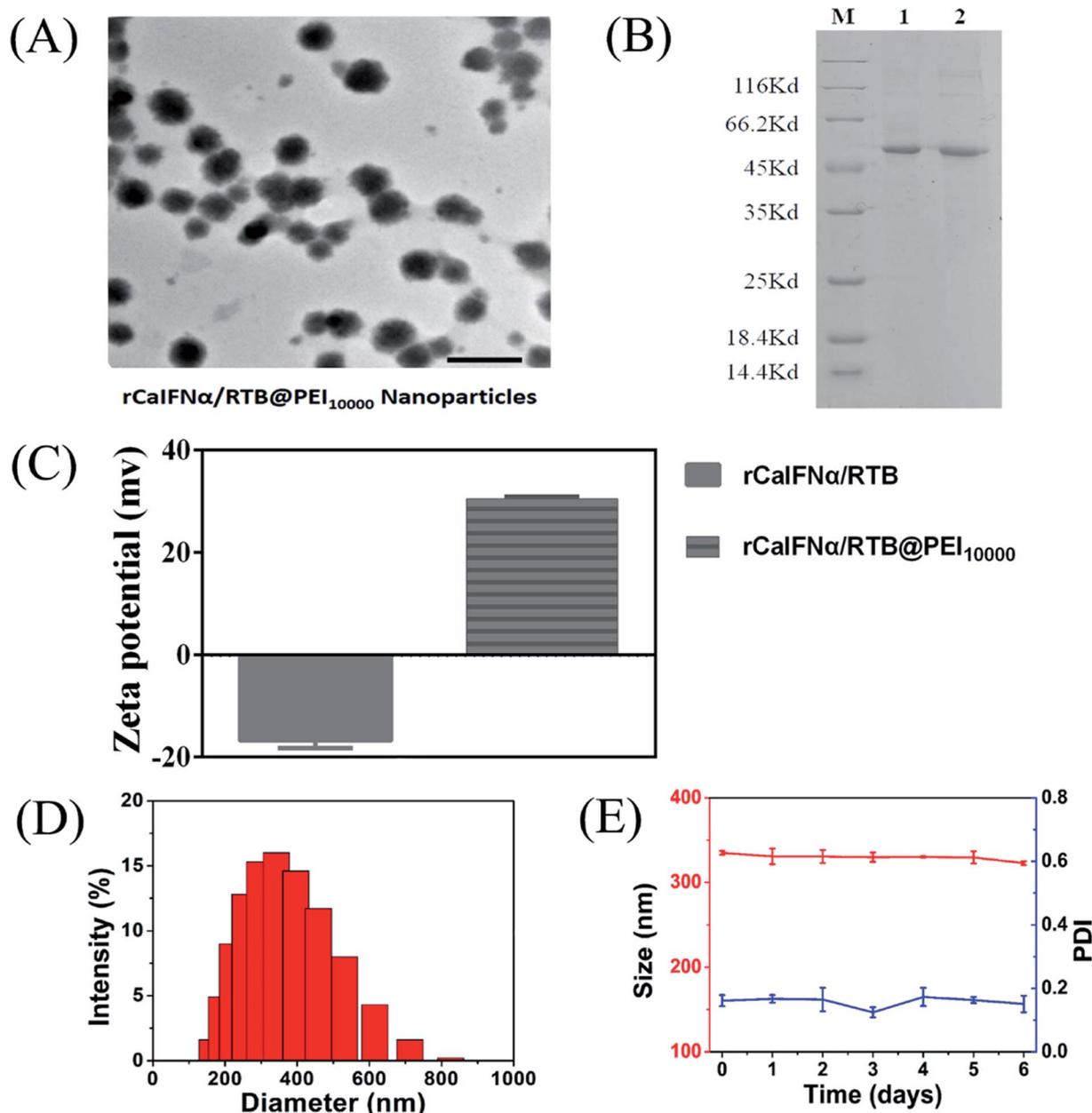Fig. 4 (A) TEM image of rCaIFNα/RTB@PEI$_{10000}$; the scale bar indicates 500 nm. (B) SDS–PAGE analysis of rCaIFNα/RTB@PEI$_{10000}$: lane 1, free rCaIFNαRTB as a control; lane 2, rCaIFNα/RTB@PEI$_{10000}$. (C) Zeta potential of rCaIFNα/RTB and rCaIFNα/RTB@PEI$_{10000}$. (D) Size distribution of rCaIFNα/RTB@PEI$_{10000}$. (E) Size change of rCaIFNα/RTB@PEI$_{10000}$ in aqueous solution at 4 °C for 6 days.

NPs by cells, and Hoechst 33258 was used as the nuclear dye (Fig. 5). First, we diluted FITC-rCaIFNα/RTB@PEI$_{10000}$ NPs (rCaIFNα/RTB: 50 μg mL^{-1}). After incubation with MDCK cells for 2 h, we found that NPs could barely enter the cell membrane; the rCaIFNα/RTB@PEI$_{10000}$ nanoparticles disintegrated, and rCaIFNα was slowly released. The uptake behavior showed a time-dependent manner. To determine whether the released rCaIFNα/RTB could be combined with cell membrane surface receptor IFNARs and activate the downstream cascade, the cell membrane dye Dil was used to locate the cell membrane. The results showed that after 2 hours of incubation, the uptake of rCaIFNα/RTB occurred. The green fluorescence signal of FITC-

rCaIFNα/RTB was overlapped by the red fluorescence signal of the cell membrane around the blue nucleus, indicating that the rCaIFNα/RTB released from NPs combined with the cell surface receptors, and the NPs were able to develop their antiviral effect through the IFNAR-JAK-STAT signaling cascade. The above results illustrate that rCaIFNα/RTB@PEI$_{10000}$ NPs have a sustained-release effect, which can prolong the half-life of the drug and better enable its biological role.

Antiviral activity of rCaIFNα/RTB and rCaIFNα/RTB@PEI$_{10000}$

To analyze the antiviral activity of rCaIFNα/RTB and rCaIFNα/RTB@PEI$_{10000}$, cytopathic inhibition assay was operated with
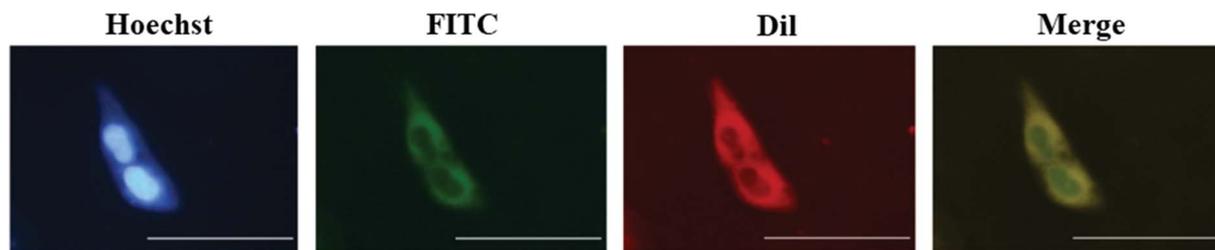
Fig. 5 Fluorescence imaging of MDCK cells incubated with FITC–rCaIFNα/RTB@PEI$_{10000}$ NPs for 2 hours; the scale bar indicates 100 μm.

MDCKs, and the antiviral activity of rCaIFNα/RTB and rCaIFNα/RTB@PEI$_{10000}$ was analysed and compared with commercial CaIFNα (Fig. 6). rCaIFNα/RTB and rCaIFNα/RTB@PEI$_{10000}$ were serially diluted and pre-incubated with MDCKs for 24 h, then 100× TCID$_{50}$ VSV was challenged for another 24 h. Results show that while the viral control displayed complete cytopathicity, the rCaIFNα/RTB and rCaIFNα/RTB@PEI$_{10000}$ protein exerted a superior antiviral activity compared to commercial CaIFNα. The recombinant fusion protein and its NPs were able to develop protective effects with the MDCK cell line from the 100× TCID$_{50}$ VSV challenges. The antiviral activity against VSV reached 1.2×10^9 IU mL^{-1} with the recombinant protein concentration at 1.4 mg mL^{-1}. We also conducted a cytopathic inhibition assay with WISH cell lines, but results show that the recombinant fusion protein could not develop its antiviral activity in WISH cell lines, mainly because the antiviral ability of rCaIFNα/RTB was species-specific.

Primary physicochemical characteristics of rCaIFNα/RTB and rCaIFNα/RTB@PEI$_{10000}$

We tested the stability of rCaIFNα/RTB and rCaIFNα/RTB@PEI$_{10000}$ at pH 2, 4, 6, 7, 9, and 11, as well as at 42 °C, 56 °C, and 65 °C, respectively. Therefore, rCaIFNα/RTB was treated at different conditions, then antiviral assay was conducted in the MDCK/VSV system in parallel for rCaIFNα/RTB and rCaIFNα/RTB@PEI$_{10000}$. Results showed that rCaIFNα/RTB and rCaIFNα/RTB@PEI$_{10000}$ were stable at changing pH conditions, but when incubated in 65 °C for 4 h, the rCaIFNα/RTB antiviral activity was lost, but that of rCaIFNα/RTB@PEI$_{10000}$

was not (Fig. 7A and B). In addition, physicochemical characteristics of rCaIFNα/RTB were analyzed using the MDCK/VSV system, including pH and temperature sensitivity. rCaIFNα/RTB was verified to be sensitive to temperature and pH variation, but after rCaIFNα/RTB was assembled with the polyethylenimine polymer, the rCaIFNα/RTB@PEI$_{10000}$ was remarkably stable at various temperature and pH levels. Given the substantial antiviral activity and low cytotoxicity of rCaIFNα/RTB@PEI$_{10000}$, it is a potential candidate for a novel, effective therapeutic agent.

Conclusion

In conclusion, a novel fusion protein rCaIFNα/RTB was expressed, and its biological activity was estimated. rCaIFNα/RTB presented moderate biological activity and low cytotoxicity. This research provides a new idea and developed direction for the biological modification of canine interferon α, and it demonstrates a new proof that biotoxin subunits can be used as an excellent carrier protein. Furthermore, rCaIFNα/RTB@PEI$_{10000}$ NPs were synthesized, and their biological activities were estimated as well. The NPs enhance the stability of rCaIFNα/RTB and enable greater tolerance to pH and temperature, while maintaining significant antiviral activity in extremely acidic conditions. This work provides a new idea for the study of new dosage forms of canine interferon α and shows the great potential of PEI$_{10000}$ as a simple and effective nano-drug carrier in the study of drug stability. All of these findings lay a foundation for future research into rCaIFNα/RTB and
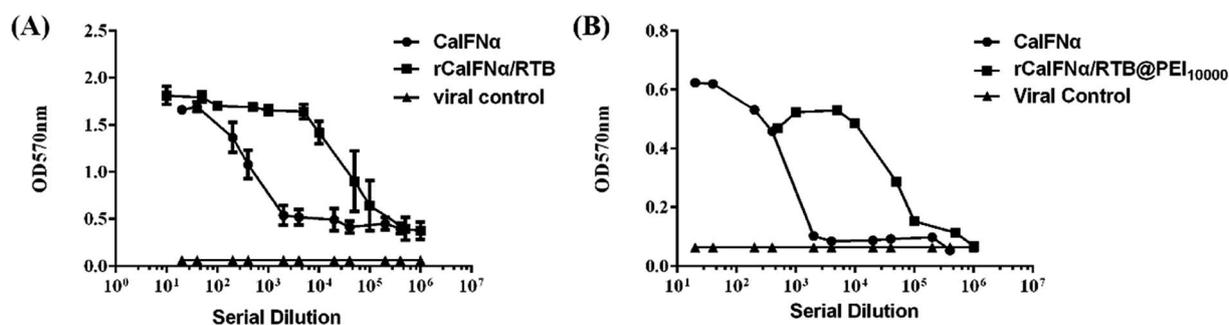

Fig. 6 Antiviral activity of (A) rCaIFNα/RTB and (B) rCaIFNα/RTB@PEI$_{10000}$. The protective effects of rCaIFNα/RTB and rCaIFNα/RTB@PEI$_{10000}$ were evaluated in antiviral assays compared with commercial CaIFNα using MDCK cell lines challenged with 100× TCID$_{50}$ VSV, as described under Materials and methods.
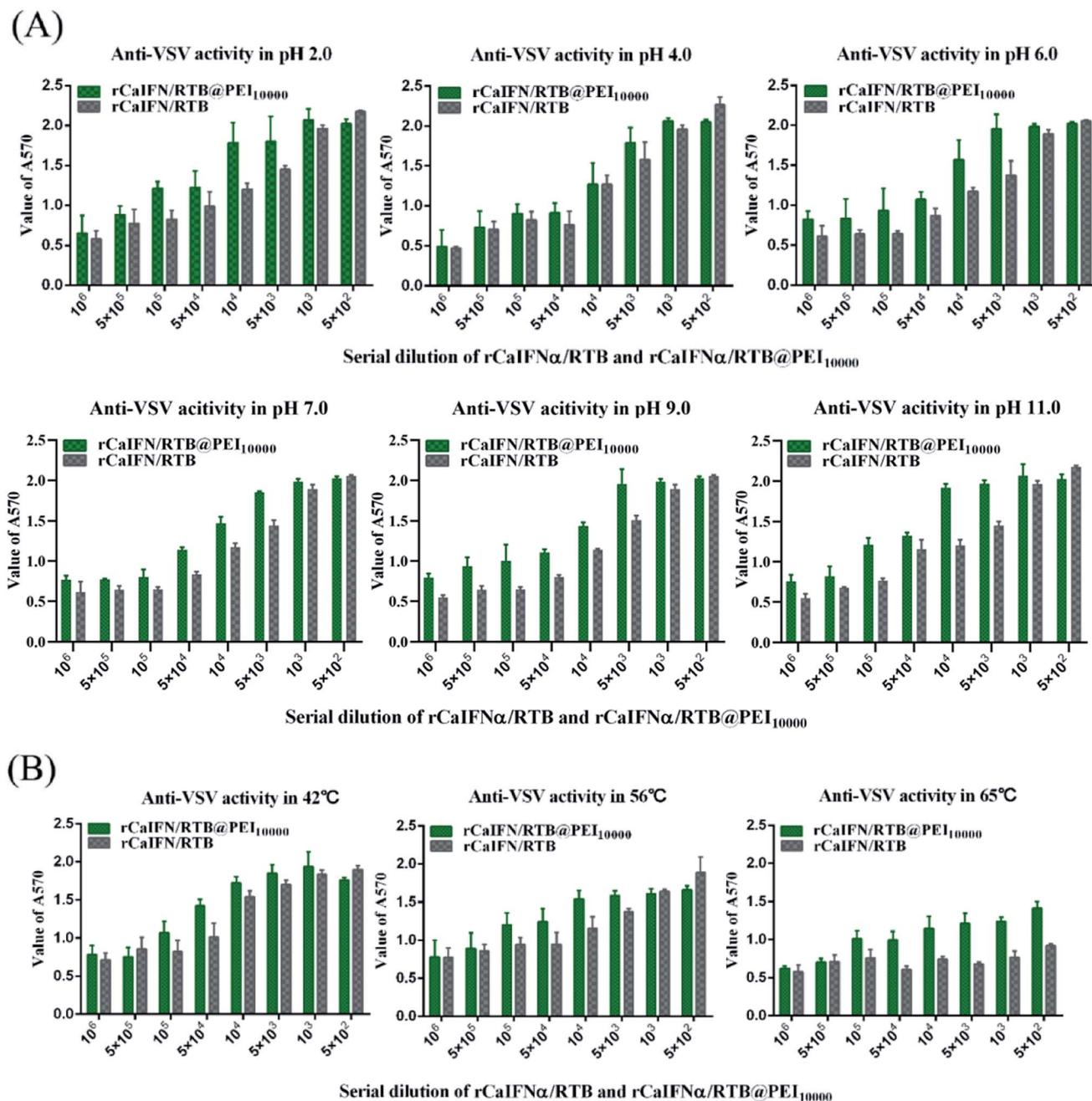
Fig. 7 Comparison of antiviral activity of rCaIFNα/RTB and rCaIFNα/RTB@PEI$_{10000}$ on MDCK cell lines challenged with 100× TCID$_{50}$ VSV after treatment at various pH conditions and temperatures.

might also provide insights on the use of rCaIFNα/RTB as an effective antiviral agent against viral dog infections and diseases.

Materials and methods

Virus and vector

Vesicular stomatitis virus (VSV) was kindly provided by Dr Zhang Guo Li from Changchun Military Veterinary Research Institute. The recombinant *E. coli* cloning vector for canine *IFNα* and *RTB* was constructed and preserved in our laboratory.

Overlap PCR method was used to link the 3′ end of the canine *IFNα* gene and 5′ end of the *RTB* gene with linker sequence, which is N-GGGGSGGGGSGGGGS-C ((G$_4$S)$_3$ linker).

Prokaryotic expression of CaIFNα/RTB and renaturation process

The recombinant cloning vector *pMD19T-CaIFNα/RTB* was digested with restriction enzymes Nde I and Xho I. The gene fragment of interest was inserted into the expression vector pET28a (Novagen, Darmstadt, Germany), which included an N-

terminal histidine hexamer tag (6×His tag). The recombinant expression vector was constructed and transformed into *E. coli*/BL21(DE3). The recombinant protein rCaIFNα/RTB was expressed mainly in the form of inclusion bodies and then resolved in denaturation buffer with a high concentration of urea. The denatured rCaIFNα/RTB was purified with chelating sepharose, which was charged with nickel and renatured in urea gradient dialysis. The final concentration of rCaIFNα/RTB was determined with the BCA protein assay and then analyzed with SDS-PAGE.

Western blot analysis of rCaIFNα/RTB

After SDS-PAGE analysis, proteins were transferred to PVDF membrane without staining. Then, the membrane was blocked with PBS containing 5% BSA. Rabbit monoclonal antibody against 6×His tag (1 : 3000 diluted) was used as the primary antibody, and HRP-conjugated goat anti-rabbit IgG (1 : 40 000 diluted) was used to detect the immune complex.

Analysis of antiviral activity *in vitro*

Antiviral activity was assayed by the ability of rCaIFNα/RTB to inhibit the cytopathic effects (CPE) of vesicular stomatitis virus (VSV) on canine kidney cells (MDCK) according to the protocols below. MDCK was purchased from the Cell Bank of the Chinese Academy of Sciences (Shanghai, China) and cultured in DMEM supplemented with 8% fetal bovine serum. Cells were digested, then seeded onto 96-well plates to a concentration of 5×10^4 cell per mL for the antiviral activity assay. Cells were treated with commercial canine IFN alpha and rCaIFNα/RTB, then filter-sterilized and serially diluted with DMEM supplemented with 2% FBS. The plates were incubated at 37 °C with 5% CO_2 for 24 h. Then, the supernatant was discarded, and cells were washed with DMEM without FBS three times and challenged with VSV (100× $TCID_{50}$). When the CPE reached 100% in the viral control, whole cells were stained with crystal violet for 30 min, then washed with ddH_2O three times. The crystal violet was eluted with 100 μL elution buffer (50% ethanol, 0.1% acetic acid), and absorbance was measured at 595 nm on a microplate reader (Tecan infinite F500). The antiviral activity of rCaIFNα/RTB was also estimated in the human amniotic cell line (WISH), cultured in DMEM supplemented with 8% FBS. All antiviral assays were repeated three times.

Detection of primary physicochemical characteristics of rCaIFNα/RTB and rCaIFNα/RTB@PEI10000

The physicochemical characteristics of rCaIFNα/RTB and rCaIFNα/RTB@PEI10000 were analyzed using the MDCK/VSV system, including pH and temperature sensitivity. In detail, the rCaIFNα/RTB and rCaIFNα/RTB samples were analyzed as follows: (1) combined with hydrogen chloride or sodium hydroxide to adjust pH levels of 2.0, 4.0, 6.0, 7.0, 9.0, 11.0 or 4 h at 4 °C, after which they were adjusted back to the original pH 7.0; (2) placed in a 42 °C, 53 °C, and 65 °C water bath for 4 h, then rapidly placed in an icebox for cooling, after which the antiviral activity was determined by the MDCK/VSV system. The antiviral activities of the rCaIFNα/RTB and rCaIFNα/RTB@PEI10000 samples were compared.

Conflicts of interest

There are no conflicts of interest to declare.

Acknowledgements

References

1 A. Isaacs and J. Lindenmann, Virus interference. I. The interferon, *Proc. R. Soc. Lond. B Biol. Sci.*, 1957, **147**(927), 258–267.

2 M. K. Crow and L. Ronnblom, Type I interferons in host defence and inflammatory diseases, *Lupus Science & Medicine*, 2019, **6**(1), e000336.

3 D. S. Aaronson and C. M. Horvath, A Road Map for Those Who Don't Know JAK-STAT, *Science*, 2002, **296**, 1653–1655.

4 N. Raftery and N. J. Stevenson, Advances in anti-viral immune defence: revealing the importance of the IFN JAK/STAT pathway, *Cell. Mol. Life Sci.*, 2017, **74**(14), 2525–2535.

5 W. M. Schneider, M. D. Chevillotte and C. M. Rice, Interferon-Stimulated Genes: A Complex Web of Host Defenses, *Annu. Rev. Immunol.*, 2014, **32**(1), 513–545.

6 S. Nagata, Restoration of antibody forming capacity in early-thymectomized Xenopus by injecting thymocytes, *Dev. Comp. Immunol.*, 1980, **4**(3), 553–557.

7 A. Domenech, G. Miro, V. M. Collado, N. Ballesteros, L. Sanjose, E. Escolar, S. Martin and E. Gomez-Lucia, Use of recombinant interferon omega in feline retrovirosis: from theory to practice, *Vet. Immunol. Immunopathol.*, 2011, **143**(3–4), 301–306.

8 E. Sagnelli, M. Pisaturo, S. Martini, C. Sagnelli, P. Filippini and N. Coppola, Advances in the treatment of hepatitis B virus/hepatitis C virus coinfection, *Expet Opin. Pharmacother.*, 2014, **15**(10), 1337–1349.

9 A. Sanchez, M. Tobio, L. Gonzalez, A. Fabra and M. J. Alonso, Biodegradable micro- and nanoparticles as long-term delivery vehicles for interferon-alpha, *Eur. J. Pharm. Sci.*, 2003, **18**(3–4), 221–229.

10 J. Qiu, X. H. Wei, F. Geng, R. Liu, J. W. Zhang and Y. H. Xu, Multivesicular liposome formulations for the sustained delivery of interferon alpha-2b, *Acta Pharmacol. Sin.*, 2005, **26**(11), 1395–1401.

11 H. J. Flink, M. van Zonneveld, B. E. Hansen, R. A. de Man, S. W. Schalm, H. L. Janssen and H. B. V. S. Group, Treatment with Peg-interferon alpha-2b for HBeAg-positive chronic hepatitis B: HBsAg loss is associated with HBV genotype, *Am. J. Gastroenterol.*, 2006, **101**(2), 297–303.

12 A. Maughan and O. Ogbuagu, Pegylated Interferon Alpha 2a for the Treatment of Hepatitis C Virus Infection, *Expet Opin. Drug Metabol. Toxicol.*, 2018, **14**(2), 219–227.

13 V. G. Bain, K. D. Kaita, E. M. Yoshida, M. G. Swain, E. J. Heathcote, A. U. Neumann, M. Fiscella, R. Yu, B. L. Osborn, P. W. Cronin, W. W. Freimuth, J. G. McHutchison and G. M. Subramanian, A phase 2 study to evaluate the antiviral activity, safety, and pharmacokinetics of recombinant human albumin-interferon alfa fusion protein in genotype 1 chronic hepatitis C patients, *J. Hepatol.*, 2006, **44**(4), 671–678.

14 B. L. Osborn, H. S. Olsen, B. Nardelli, J. H. Murray, J. X. H. Zhou, A. Garcia, G. Moody, L. S. Zaritskaya and C. Sung, Pharmacokinetic and Pharmacodynamic Studies of a Human Serum Albumin-Interferon-α Fusion Protein in Cynomolgus Monkeys, *J. Pharmacol. Exp. Therapeut.*, 2002, **303**, 540–548.

15 J. Audi, M. Belson, M. Patel, J. Schier and J. Osterloh, Ricin poisoning: a comprehensive review, *JAMA*, 2005, **294**(18), 2342–2351.

16 A. Rapak, P. O. Falnes and S. Olsnes, Retrograde transport of mutant ricin to the endoplasmic reticulum with subsequent translocation to cytosol, *Proc. Natl. Acad. Sci. U. S. A.*, 1997, **94**(8), 3783–3788.

17 K. Sandvig and B. van Deurs, Delivery into cells: lessons learned from plant and bacterial toxins, *Gene Ther.*, 2005, **12**(11), 865–872.

18 N. W. Choi, M. K. Estes and W. H. Langridge, Mucosal immunization with a ricin toxin B subunit-rotavirus NSP4 fusion protein stimulates a Th1 lymphocyte response, *J. Biotechnol.*, 2006, **121**(2), 272–283.

19 A. Firsov, I. Tarasenko, T. Mitiouchkina, L. Shaloiko, O. Kozlov, L. Vinokurov, E. Rasskazova, A. Murashev, A. Vainstein and S. Dolgov, Expression and Immunogenicity of M2e Peptide of Avian Influenza Virus H5N1 Fused to Ricin Toxin B Chain Produced in Duckweed Plants, *Front. Chem.*, 2018, **6**, 22.

20 F. Medina-Bolivar, R. Wright, V. Funk, D. Sentz, L. Barroso, T. D. Wilkins, W. Petri Jr and C. L. Cramer, A non-toxic lectin for antigen delivery of plant-based mucosal vaccines, *Vaccine*, 2003, **21**(9–10), 997–1005.

21 L. Ou, M. J. Przybilla, B. Koniar and C. B. Whitley, RTB lectin-mediated delivery of lysosomal alpha-l-iduronidase mitigates disease manifestations systemically including the central nervous system, *Mol. Genet. Metab.*, 2018, **123**(2), 105–111.

22 A. Singh, S. Srivastava, A. Chouksey, B. S. Panwar, P. C. Verma, S. Roy, P. K. Singh, G. Saxena and R. Tuli, Expression of rabies glycoprotein and ricin toxin B chain (RGP-RTB) fusion protein in tomato hairy roots: a step towards oral vaccination for rabies, *Mol. Biotechnol.*, 2015, **57**(4), 359–370.

23 N. Xu, H. Yuan, W. Liu, S. Li, Y. Liu, J. Wan, X. Li, R. Zhang and Y. Chang, Activation of RAW264.7 mouse macrophage cells in vitro through treatment with recombinant ricin toxin-binding subunit B: involvement of protein tyrosine, NF-kappaB and JAK-STAT kinase signaling pathways, *Int. J. Mol. Med.*, 2013, **32**(3), 729–735.

24 W. T. Godbey, K. K. Wu and A. G. Mikos, Poly(ethylenimine) and its role in gene delivery, *J. Controlled Release*, 1999, **60**(2–3), 149–160.

25 S. Kumar, S. Raj, K. Sarkar and K. Chatterjee, Engineering a multi-biofunctional composite using poly(ethylenimine) decorated graphene oxide for bone tissue regeneration, *Nanoscale*, 2016, **8**(12), 6820–6836.

26 T. Gonzalez-Fernandez, B. N. Sathy, C. Hobbs, G. M. Cunniffe, H. O. McCarthy, N. J. Dunne, V. Nicolosi, F. J. O'Brien and D. J. Kelly, Mesenchymal stem cell fate following non-viral gene transfection strongly depends on the choice of delivery vector, *Acta Biomater.*, 2017, **55**, 226–238.

27 B. Gurumurthy, P. C. Bierdeman and A. V. Janorkar, Spheroid model for functional osteogenic evaluation of human adipose derived stem cells, *J. Biomed. Mater. Res., Part A*, 2017, **105**(4), 1230–1236.

28 X. Ye, S. Li, X. Chen, Y. Zhan and X. Li, Polyethylenimine/silk fibroin multilayers deposited nanofibrics for cell culture, *Int. J. Biol. Macromol.*, 2017, **94**(pt A), 492–499.

29 S. Dong, X. Zhou and J. Yang, TAT modified and lipid–PEI hybrid nanoparticles for co-delivery of docetaxel and pDNA, *Biomed. Pharmacother.*, 2016, **84**, 954–961.

30 Y. Li, M. Guo, Z. Lin, M. Zhao, M. Xiao, C. Wang, T. Xu, T. Chen and B. Zhu, Polyethylenimine-functionalized silver nanoparticle-based co-delivery of paclitaxel to induce HepG2 cell apoptosis, *Int. J. Nanomed.*, 2016, **11**, 6693–6702.

31 F. Oroojalian, A. H. Rezayan, W. T. Shier, K. Abnous and M. Ramezani, Megalin-targeted enhanced transfection efficiency in cultured human HK-2 renal tubular proximal cells using aminoglycoside-carboxyalkyl- polyethylenimine -containing nanoplexes, *Int. J. Pharm.*, 2017, **523**(1), 102–120.

32 S. T. Pang, F. W. Lin, C. K. Chuang and H. W. Yang, Co-Delivery of Docetaxel and p44/42 MAPK siRNA Using PSMA Antibody-Conjugated BSA-PEI Layer-by-Layer Nanoparticles for Prostate Cancer Target Therapy, *Macromol. Biosci.*, 2017, **17**(5), 1600421.

33 X. Chen, J. L. Zaro and W. C. Shen, Fusion protein linkers: property, design and functionality, *Adv. Drug Deliv. Rev.*, 2013, **65**(10), 1357–1369.

34 J. S. Klein, S. Jiang, R. P. Galimidi, J. R. Keeffe and P. J. Bjorkman, Design and characterization of structured protein linkers with differing flexibilities, *Protein Eng. Des. Sel.*, 2014, **27**(10), 325–330.

35 V. P. Reddy Chichili, V. Kumar and J. Sivaraman, Linkers in the structural biology of protein-protein interactions, *Protein Sci.*, 2013, **22**(2), 153–167.

36 S. Liu, D. Zhou, J. Yang, H. Zhou, J. Chen and T. Guo, Bioreducible Zinc(II)-Coordinative Polyethylenimine with Low Molecular Weight for Robust Gene Delivery of Primary and Stem Cells, *J. Am. Chem. Soc.*, 2017, **139**(14), 5102–5109.

37 P. C. Pandey, G. Pandey and R. J. Narayan, Polyethylenimine-mediated synthetic insertion of gold nanoparticles into mesoporous silica nanoparticles for drug loading and biocatalysis, *Biointerphases*, 2017, **12**(1), 011005.

38 D. Shao, H. Wu, F. Shen, H. Wu and J. Quan, Carbon dioxide-modified polyethylenimine as a novel gene delivery vector and its in vitro validation, *J. Biomater. Appl.*, 2017, **31**(9), 1257–1266.

39 H. Wang, Y. Li, M. Zhang, D. Wu, Y. Shen, G. Tang and Y. Ping, Redox-Activatable ATP-Depleting Micelles with Dual Modulation Characteristics for Multidrug-Resistant Cancer Therapy, *Adv. Healthcare Mater.*, 2017, **6**(8), 1601293.

40 B. Yang, X. Ni, L. Chen, H. Zhang, P. Ren, Y. Feng, Y. Chen, S. Fu and J. Wu, Honokiol-loaded polymeric nanoparticles: an active targeting drug delivery system for the treatment of nasopharyngeal carcinoma, *Drug Deliv.*, 2017, **24**(1), 660–669.